ELSEVIER

Journal of Neuroscience Methods 167 (2008) 384–392

JOURNAL OF NEUROSCIENCE METHODS

www.elsevier.com/locate/jneumeth

A semi-automated algorithm for studying neuronal oscillatory patterns: A wavelet-based time frequency and coherence analysis

Rodrigo N. Romcy-Pereira [a,*], Draulio B. de Araujo [b,**], João P. Leite [a], Norberto Garcia-Cairasco [a]

[a] *Ribeirão Preto School of Medicine, University of São Paulo, Ribeirão Preto, SP, Brazil*
[b] *Department of Physics and Mathematics, University of São Paulo, Ribeirão Preto, SP, Brazil*

Received 15 May 2007; received in revised form 24 August 2007; accepted 28 August 2007

Abstract

In many experimental designs, animal observation is associated with local field potential (LFP) recordings in order to find correlations between behavior dynamics and neuronal activity. In such cases, relevant behaviors can occur at different times during free-running recordings and should be put together by the time of analysis. Here, we developed a MATLAB semi-automated toolbox to quantitatively analyze the temporal progression of brain oscillatory activity in multiple free-running LFP recordings obtained during spontaneous behaviors. The algorithm works by selecting LFP epochs at user-defined onset times (locked to behavior, drug injection time, etc.), calculates their time–frequency spectra, detects long-lasting oscillatory events and calculates linear coherence between pair of electrodes. As output, it generates several table-like text and tiff image files, besides group descriptive statistics. To test the algorithm, we recorded hippocampus and amygdala LFPs from rats in different behavioral states: awake (AW), sleep (SWS, slow-wave sleep and REMS, rapid-eye movement sleep) and tonic–clonic seizures. The results show that the software reliably detects all oscillatory events present in up to seven user-defined frequency bands including onset/offset time and duration. It also calculates the global spectral composition per epoch from each subject and the linear coherence (with confidence intervals) as a measure of spectral synchronization between brain regions. The output files provide an easy way to do within-subject as well as across-subject analysis. The routines will be freely available for downloading from our website http://www.neuroimago.usp.br/BPT/.

Keywords: Quantitative EEG analysis; Time–frequency analysis; Epilepsy; Sleep; Hippocampus; Amygdala

1. Introduction

Brain oscillatory activity is a property of both local and distributed neural networks found in cortical/sub-cortical circuitries (Cantero and Atienza, 2005). It is commonly generated by the coordinated activity of interconnected excitatory and inhibitory neurons, which produce regular oscillations of field extracellular potentials. Distinct oscillatory patterns are associated to different physiological states (awake, sleep, sedation), perceptual representations (visual, auditory) and cognitive processes (attention, learning and memory) (Cantero and Atienza, 2005; Gross et al., 2001; Steriade, 1997).

The correlation between a neurophysiological measurement and a behavioral response has shown to be a successful and productive approach to investigate the neural networks underlying many behaviors (Jensen et al., 2002; Makeig et al., 2004). However, it is deeply dependent on the availability of objective and quantitative analytical methods to handle and extract the relevant information from the experimental data. It requires automated algorithms to deal with a large amount of recordings that usually contain a high degree of redundancy and eventual artifacts.

The implantation of microelectrodes for local field potential (LFP; or deep EEG) recordings in rodents is a widely used electrophysiological technique to measure the electrical activity state of a brain region and is often used to correlate neural circuitry

Abbreviations: AW, awake; bTFR, binarized time–frequency representation; EEG, electroencephalogram; LFP, local field potential; REMS, rapid-eye movement sleep; STFT, short-time Fourier transform; SWS, slow-wave sleep; TFR, time–frequency representation.

* Corresponding author at: University of São Paulo, Av. Bandeirantes, 3900, Ribeirão Preto, SP 14049-900, Brazil. Tel.: +55 16 602 2556/4535.
** Corresponding author at: University of São Paulo, Av. Bandeirantes, 3900, Ribeirão Preto, SP 14049-900, Brazil. Tel.: +55 16 3602 3822/778.
E-mail addresses: rnrpereira@rnp.fmrp.usp.br (R.N. Romcy-Pereira), draulio@biomag.usp.br (D.B. de Araujo).

0165-0270/$ – see front matter © 2007 Elsevier B.V. All rights reserved.
doi:10.1016/j.jneumeth.2007.08.027

activation and behavior. As LFPs and behaviors are intrinsically dynamic variables, they require analytical tools that preserve their temporal information. LFPs are locally recorded and can be partially characterized by their frequency components and associated durations. Similarly, behaviors change with time and therefore, they have duration. However, the animal's phenotypic expression is a qualitative categorical variable.

Different methods can be used to obtain the spectral decomposition of a signal (Drongelen, 2006). In contrast to the traditional Fourier transform, the spectral analysis using the wavelet transform presents several advantages regarding the combined study of the time and frequency domains. Importantly, it presents a better resolution trade-off between the spectral decomposition of LFPs calculated at each time point than the Fourier analog, the Short-Time Fourier Transform (STFT) (Tallon-Baudry et al., 1997). Moreover, the most commonly used quantitative output parameters calculated are the oscillating frequency at a certain time and its spectral power. In many instances when two or more signals are analyzed, the coherence function is calculated to estimate the degree of linear correlation between the signals at specific frequencies (Challis and Kitney, 1991).

Our laboratory has traditionally studied the behavioral expression of epileptic seizures by analyzing the interaction between behavioral components during ictal episodes (Dal-Cól et al., 2006; Garcia-Cairasco et al., 1996). The introduction of the simultaneous recording of LFPs and ictal behaviors through video-EEG recordings prompted us to develop an analytical tool to evaluate the spectral time course of specific behaviors. To put LFPs and behaviors together, we decided to use a time–frequency spectral analysis using the wavelet transform and calculate useful quantitative output parameters such as the sustained frequency (onset, offset and duration) that could be correlated with the annotated behaviors. Some of these parameters had already been used in the literature (Drongelen, 2006). Therefore, we present here an easy to use and freely available algorithm able to extract epochs from multiple full-length files, to help the user to exclude epochs with artifacts and to calculate the time-varying power spectra on a large set of data. The algorithm was tested in well-known datasets whose behaviors were previously determined.

2. Materials and methods

2.1. Algorithm

All routines were written in Matlab 6.5 R13 (Mathworks Inc, MA, USA). The algorithm consists of five steps and routine names are shown in parenthesis.

I Epoch Selection, Extraction and Artifact Rejection (*epoch_select* and *epoch_display*).
II Wavelet Time–Frequency Analysis (*timefreq_sust*).
III Calculation of Sustained Oscillations and Frequency Peaks (*timefreq_sust*).
IV Calculation of Across-Subjects Statistics (*analysis*).
V Calculation of Coherence and Confidence Intervals (*cohereboot*).

2.1.1. Epoch selection, extraction and artifact rejection

The first step of the analysis consists in processing the behavior timetable data. Based on the timetable obtained during the observation of animal's performance, the experimenter will define relevant LFP segments to be analyzed. The routine *epoch_select* reads LFP recordings as text files and generates fixed-length epoch files at user-defined onset times. The routine *epoch_display* displays extracted epochs on the computer screen for visual inspection. By checking all epoch segments on the computer screen, the user can exclude artifact-containing files from the working folder and proceed with the analysis. It is important to stress that epoch extraction is a fully automated task and can be used on multiple files. Artifact rejection has to be done manually.

Input parameters: dataset name, epoch duration, onset times. Output: epoch text files, matlab figure and tiff image with all extracted epochs to be displayed on the computer screen.

2.1.2. Wavelet time–frequency analysis

Time–frequency representation (TFR) of biological signals has important applications in the study of behavioral dynamics. The most intuitive form to simultaneously accomplish time and frequency analysis of a signal is to segment the time series into small fragments (windows) and calculate their spectrum, the so-called Short-Time Fourier Transform (STFT):

$$\mathrm{STFT}(t,\omega) = \int [x(\tau) - W(\tau - t)]\, \mathrm{e}^{-\mathrm{j}\omega\tau}\, \mathrm{d}\tau,$$

where W is the sliding window used to segment the signal.

By computing the STFT of a signal, also known as spectrogram, a power spectrum is obtained for different displacements in time t, segmented by the window W. The spectrogram shows how the energy of the signal is distributed both in time and in frequency and, is typically visualized as an image. In such analysis, the size and type of the chosen window is of fundamental importance. However, as the resolution in time increases (i.e., the length of W decreases), one loses accuracy in the frequency component. Such limitation of the STFT gave rise to the development of alternatives, such as the Wavelet analysis. This method provides a better compromise between time and frequency resolution (Jensen et al., 2002; Tallon-Baudry et al., 1997).

Wavelets are mathematical functions, $\psi(t)$ that satisfy specific requirements. They should (1) decay rapidly as $t \to \pm\infty$, (2) be zero mean, and (3) have a Fourier transform, $\hat{\psi}(\omega)$ that obeys the following condition:

$$\int_0^{+\infty} \frac{|\hat{\psi}(\omega)|^2}{\omega}\, \mathrm{d}\omega = \int_{-\infty}^{0} \frac{|\hat{\psi}(\omega)|^2}{|\omega|}\, \mathrm{d}\omega = C_\psi < +\infty$$

There are many types of wavelets, also known as basis. In this study, we used Morlet wavelet basis for calculating TFRs according to the expression:

$$w(f_0, t) = A_\varphi \cdot \mathrm{e}^{-t^2/2\sigma_t^2} \cdot \mathrm{e}^{\mathrm{i}2\pi f_0 t},$$

where $\sigma_t = 1/2\pi\sigma_f$ is the time of the wavelet and σ_f is its frequency.

The energy of a signal $s(t)$, in a specific frequency band f_0, can be obtained by the convolution:

$$E(t, f_0) = |w(t, f_0) \otimes s(t)|^2$$

As a result, we obtain the energy content of the signal (e.g., LFP epoch) at a specific time and frequency: an m (time) $\times$ n (frequency) matrix. The output can be visualized as an image, where the pixel intensity represents energy and the x–y frame represents the time and frequency, respectively.

Input parameters necessary for the analysis: LFP epochs (datasets), LFP sampling rate (***Fs***), lower limit frequency ($\boldsymbol{f_0}$), frequency resolution ($\Delta \boldsymbol{f}$) and upper limit frequency ($\boldsymbol{f_f}$).

2.1.3. Calculation of sustained oscillations and frequency peaks

Individual TFR images are initially binarized to produce a black-and-white TFR image (bTFR) and then, subjected to a sliding-window algorithm that extracts sustained oscillations. Binarization is accomplished by using Otsu's thresholding method implemented in a matlab routine (*imadjust, graythresh*) and its reliability was checked through the comparison of various TFRs and bTFRs (Otsu, 1979). The sliding window algorithm was designed to sweep bTFR images and extract oscillations lasting $\geq$ 600 ms, at seven preset frequency bands with a time resolution of 200 ms. In addition, the user can choose to merge adjacent oscillations separated by a predefined time gap. Oscillatory events are saved as a text file in a table-like format containing the following information: epoch number, frequency range ($\boldsymbol{F}_{\text{range}}$; e.g., 1–5 Hz), onset time ($\boldsymbol{T}_0$), offset time ($\boldsymbol{T}_f$) and duration (in s). In addition, it calculates the global power spectrum of each epoch and generates a second output text file containing epoch number, peak frequencies (Hz) and power at peak frequencies (μV^2/Hz).

Input parameters: dataset name, lower and upper limits for seven frequency bands. Output: oscillatory events text file, frequency peaks text file, TFR tiff images.

2.1.4. Calculation of across-subjects statistics

Once sustained oscillations have been identified for each subject, the *analysis* routine reads them all and analyzes oscillatory events longer than a new user-defined duration (e.g., 1.5 s) considering a minimum of 600 ms. As output, it saves a text file with the descriptive statistics of each group including number of subjects analyzed, number of epochs analyzed per subject, number of oscillatory events detected per frequency band in each epoch, mean number of oscillatory events per frequency band of each subject, mean percentage (and standard deviation) of oscillatory events per frequency band across all animals. It allows the user to explore the large-scale tendency of the group at the same time it maintains individual epoch data of all subjects.

Input parameters: threshold for oscillation detection (**thre**), sustained oscillation text files from all subjects (calculated by *timefreq_sust* routine). Output: text file in table-like format.

2.1.5. Calculation of coherence and confidence intervals

The coherence function measures the linear correlation between two signals in the frequency domain (Challis and Kitney, 1991). It can be defined as the cross-spectrum modulus normalized by the auto-spectra product of two signals:

$$C_{xy}(f) = \frac{|P_{xy}(f)|^2}{P_{xx}(f)P_{yy}(f)},$$

where $C_{xy}(f)$ is the calculated coherence, $P_{xy}(f)$ the cross-spectrum of x and y signals and $P_{xx}(f)$, $P_{yy}(f)$ are the power spectrum of x and y, respectively. In addition, the phase angle delay (Φ_{xy}) between signals at each frequency can be calculated as,

$$\Phi_{xy}(f) = \arctan\left[\frac{\text{im}(P_{xy})}{\text{real}(P_{xy})]}\right],$$

where im(P_{xy}) and real(P_{xy}) are the imaginary and real parts of $P_{xy}(f)$, respectively.

Coherence is used to estimate the degree of synchronization, in the frequency domain, between two signals and its values are normalized to fit in the [0, 1] interval. Zero coherence means that the two signals are completely desynchronized, while unit coherence means the two signals are in perfect synchrony. Here, we incorporated a freely available code for the calculation of coherence and confidence intervals using a bootstrap technique (Kaplan, 2004; Zoubir and Iskander, 2004). Bootstrap creates a set of surrogate data that mimics the original data but that is completely uncoupled to them. It is accomplished by randomly permuting, in temporal order, samples from one of the signals and calculating coherence functions for each pair of surrogate and non-permuted data. In this way, the temporal structure of one data set is destroyed, while the other data set remains unchanged. The surrogate data keep the same mean, variance and histogram distribution as the original signal. After repeating this process hundreds of times, significance levels are generated at each frequency f, from the distribution of coherence estimates. In summary, we determine a threshold that defines whether the coherence between two signals is significant or not, at each specific frequency analyzed (Faes et al., 2004).

Input parameters for the coherence analysis: dataset name, epoch files (2 channel epochs—multiple epoch input through pop-up window), number of bootstrap iterations (**boot**; default: 200), LFP sampling rate ($\boldsymbol{F}_s$), confidence interval for coherence calculation (**ci**; default: 0.95). Output: Coherence and phase delay graphs saved as two matlab figures and two tiff images.

2.2. Testing the algorithm

Adult male Wistar ($n = 1$) and Wistar Audiogenic rats (WARs; $n = 6$) were individually housed in standard rodent cages and maintained at 24 °C on a 12 h light/12 h dark cycle—lights on at 07:00 h with free access to food and water (Doretto et al., 2003). Animals were unilaterally implanted with chronic electrodes ($\phi = 0.125$ mm) in the hippocampus (Wistar rats) and in the hippocampus and amygdala (WARs) under deep anesthesia (ketamine hydrocloride: xylazine, 14:1 mg/kg/Agener Uniao, SP, Brazil and Bayer, SP, Brazil). The stereotaxic coordinates used were: hippocampus, −2.0 mm posterior to bregma, 4.7 mm lateral to midline, −7.1 mm ventral to dura-mater and amygdala, −6.3 mm posterior to bregma; 4.5 mm lateral to midline;

−4.5 mm ventral to dura-mater (Paxinos, 1997). A screw in the frontal bone served as reference electrode. Animals were kept in individual cages and allowed to recover for 5 days during which they were handled and habituated to the recording chamber. All procedures were performed according to the Brazilian Society for Neuroscience and Behavior guidelines for animal research and all efforts were made to minimize animal suffering.

In order to record different behavioral states, hippocampus and amygdala LFP recordings were coupled to video monitoring (video-EEG). Video-EEGs were recorded during 16 consecutive days inside a recording chamber. LFP recordings were amplified and digitized by using a signal conditioner (CyberAmp 320, Axon Instruments, CA, USA) and an A/D converter (Biopac Systems Inc., MP100, CA, USA) connected to a personal computer running the Acqknowledge software (Biopac Systems Inc., CA, USA). Signals were sampled at 500 Hz, amplified at 1000× and filtered between 0.1 Hz and 250 Hz. In order to reduce movement artifacts, recording cables were set up with field effect transistors (Dutra Moraes et al., 2000). For Wistar rats, behaviors were classified as awake (AW), slow-wave sleep (SWS) or rapid-eye movement sleep (REMS) based on EEG and behavioral analysis. Sleep episodes (REMS and SWS) were manually scored by a trained observer while animals had hippocampus EEG recordings and were under direct visual monitoring.

For WARs, tonic–clonic seizures were induced by high intensity sound stimulation as previously described (Romcy-Pereira and Garcia-Cairasco, 2003). Annotation tables with occurrence time of each behavior were prepared during recording hours (09:00 h–17:00 h). Ten to 30-min long LFP recordings per subject were saved as text files and organized in folders according to subject and behavioral state.

Testing the algorithm consisted in (1) extracting and selecting 10-s epochs from full LFP files at predetermined behavioral states during sleep and seizure; (2) identifying sustained oscillations, (3) identifying global power spectrum peaks, (4) generating group descriptive statistics for epileptic animals and (5) detecting significant synchronization (coherence) between hippocampus and amygdala LFP recordings during seizures. Coherence computations were done only on WAR EEG data.

3. Results

Ten-second epochs were selected from long-term LFP recordings and saved in individual text files. They were organized in individual folders according to subject and behavioral state (AW, SWS and REMS). Fig. 1A shows a set of 35 SWS epochs selected and extracted from hippocampal LFP recordings during a sleep–wake cycle. They were displayed on the computer screen for visual inspection. Subsequently, multiple artifact-free epochs were chosen through a pop-up window and submitted to the time–frequency analysis. In order to automatically detect oscillatory events, TFRs were binarized. The binarization process worked reliably for the great majority of TFR images used (Fig. 1B). As a procedure to maximize its reliability in the 1–40 Hz range, we separately binarized TFRs calculated at 1–20 Hz and at 20–40 Hz. In some cases, it was necessary to up

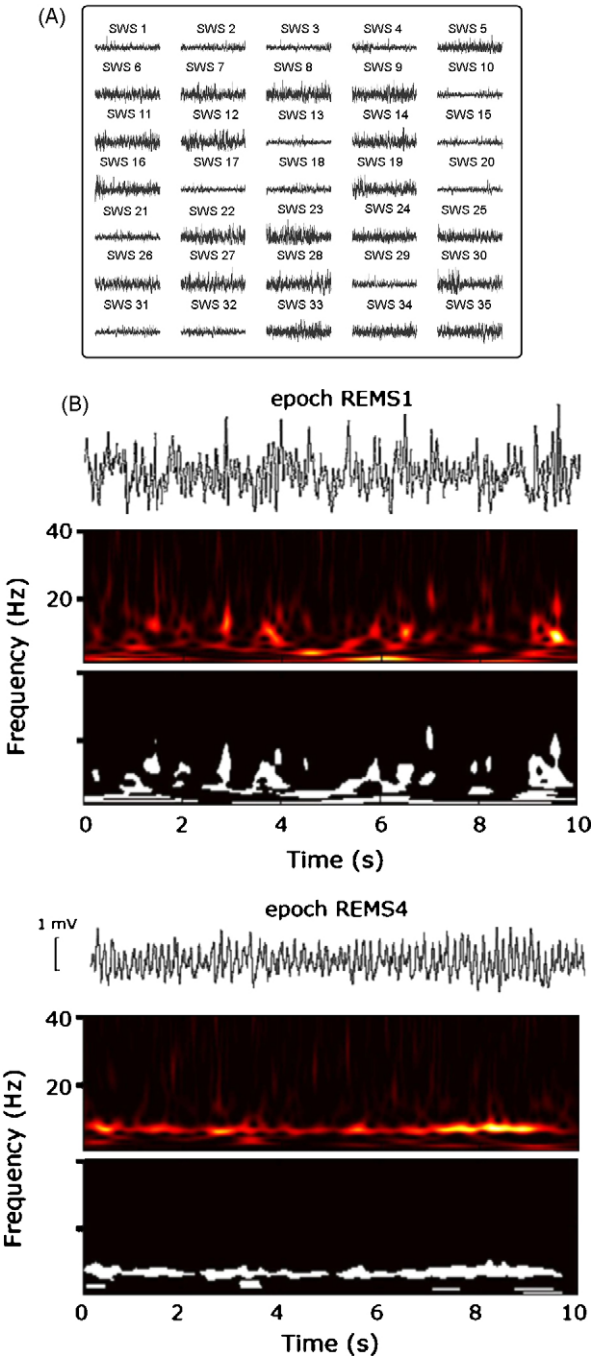

Fig. 1. (A) Epoch extraction and artifact rejection. Matlab routines read long-term LFP recordings and extract fixed-duration epochs at user-defined onset times. The selected epochs are displayed on the computer screen and become available for visual inspection. The user should exclude epochs containing artifacts from the time-frequency analysis run in the next step. Here, it is depicted a set of thirty-five SWS 10-s epochs selected from a full-length hippocampus LFP recording during sleep. (B) Time–frequency analysis and TFR binarization of REMS epochs (REMS1 and REMS4). TFR image binarization converts a continuous TFR into a 0–1 matrix, where the main oscillatory events are highlighted. Here, TFRs of two REMS 10-s epochs are shown together with their respective binarizations. Note that the binarization maintains the main oscillations whereas weaker oscillatory events are zeroed. TFR input parameters: $F_s = 500$ Hz; $f_0 = 1$ Hz, $\Delta f = 0.2$ Hz and $f_f = 40$ Hz.

Epoch	F_{range}	T_0(s)	T_f(s)	Duration (s)
1	1	0.0	2.0	2.0
1	1	4.2	6.8	2.6
1	1	8.0	9.6	1.6
1	2	3.6	4.2	0.6
1	2	5.4	7.0	1.6
1	2	9.2	10.0	0.8
1	3	1.4	2.2	0.8
1	3	6.0	6.8	0.8
1	3	9.2	10.0	0.8
2	1	1.4	3.2	1.8
2	1	3.8	4.6	0.8
2	2	2.8	3.4	0.6
3	1	0.4	2.0	1.6
3	1	3.8	5.6	1.8
3	2	4.2	5.0	0.8
3	2	5.6	10.0	4.4
4	2	0.0	9.6	9.6
5	2	1.8	5.4	3.6
5	2	6.0	8.4	2.4
6	1	8.0	8.8	0.8
6	2	0.4	2.0	1.6
6	2	3.4	6.2	2.8
6	2	7.2	8.0	0.8
6	2	8.8	9.4	0.6
7	1	2.4	3.0	0.6
7	1	7.4	8.0	0.6
7	2	0.0	9.2	9.2
8	1	1.8	2.4	0.6
8	1	4.4	7.4	3.0
8	2	0.0	2.4	2.4
8	2	3.0	5.0	2.0
8	2	6.6	7.2	0.6

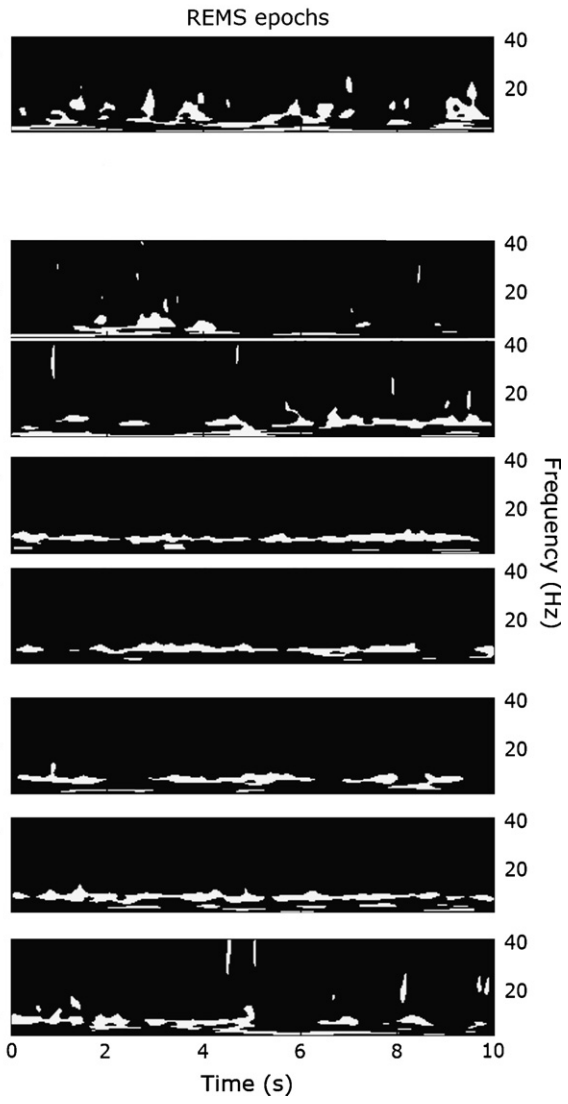

Fig. 2. Detection of sustained oscillatory events. *Left*, Oscillatory events lasting ≥600 ms were read out from REMS bTFRs and saved as a text file (table-like format). Five frequency bands (F_{range}) were analyzed: (1) 1–5 Hz; (2) 5–9 Hz; (3) 9–12 Hz; (4) 12–15 Hz; (5) 15–20 Hz, from a maximum of seven allowed. Note that ≥600 ms oscillatory events were detected in 3 frequency bands in epoch #1. Oscillations separated by a time-gap ≤600 ms were merged into one. Output file contains records of epoch number, frequency band (F_{range}), onset time (T_0), offset time (T_f) and extent (Duration) of each oscillation. *Right*, bTFRs corresponding to each epoch listed in the table on the left.

scale LFP data before TFR calculation in order to carry out the binarization. Re-scaling was applied immediately after that.

Binarized images were read out to produce a list of oscillatory events longer than 600 ms. Fig. 2 shows a table with sustained oscillations detected in 8 REMS epochs within 5 frequency bands: 1–5 Hz, 5–9 Hz, 9–12 Hz, 12–15 Hz and 15–20 Hz; and their corresponding bTFRs. In all epochs analyzed, we can see that the sliding window algorithm successfully detected all oscillatory events constrained in the user-defined frequency bands. For REMS episodes (#4–7), long-lasting oscillations in the $F_{range} = 2$ (5–9 Hz; theta band) could also be observed. Fig. 3 illustrates the global spectral composition of selected epochs from different behavioral states analyzed (AW, SWS, REMS). As expected, we could observe a prominent peak at 5–9 Hz during REMS and a low-frequency skewness of the power spectrum curve in SWS episodes. During AW, a peak at 1.6 Hz co-existed with an important contribution of frequencies higher than 5 Hz, typical of wakefulness.

EEG rythms and associated oscillatory frequency bands

EEG rhythms	Frequency band
δ (delta)	1–5 Hz
θ (theta)	5–9 Hz
α (alpha)	9–12 Hz
σ (sigma)	12–15 Hz (spindles)
β (beta)	15–30 Hz
γ (gamma)	30–40 Hz

As a necessary step in all experimental biology fields, group statistics should be produced in order to generalize individual experimental findings. Fig. 4 shows an output fragment of the across-subject descriptive statistics of sustained oscillations. Here, a new user-defined duration time threshold (e.g., 1.5 s) was established to detect oscillations present in differ-

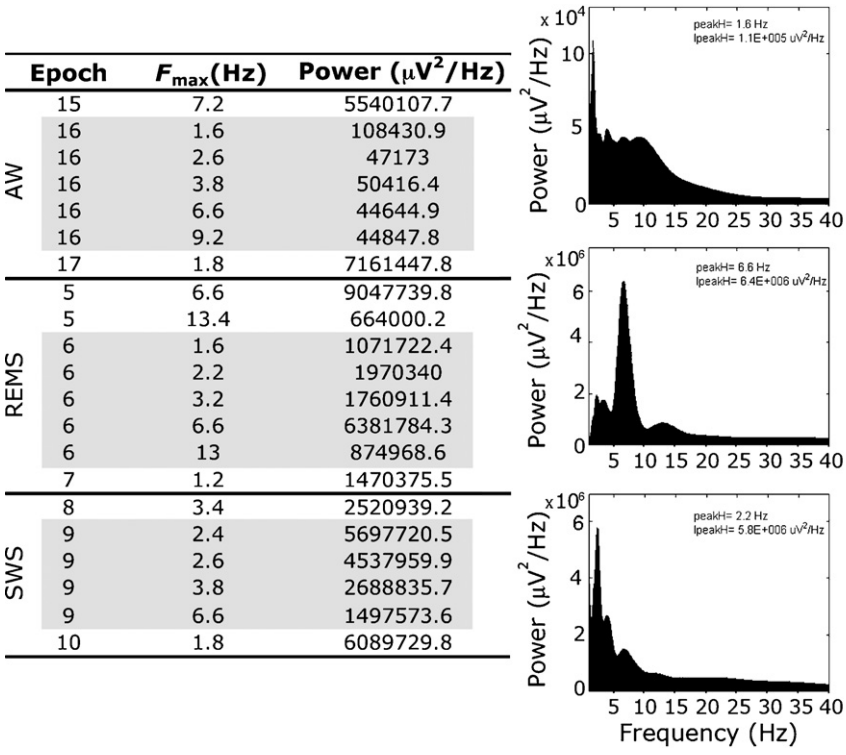

	Epoch	F_{max}(Hz)	Power (μV^2/Hz)
AW	15	7.2	5540107.7
	16	1.6	108430.9
	16	2.6	47173
	16	3.8	50416.4
	16	6.6	44644.9
	16	9.2	44847.8
	17	1.8	7161447.8
REMS	5	6.6	9047739.8
	5	13.4	664000.2
	6	1.6	1071722.4
	6	2.2	1970340
	6	3.2	1760911.4
	6	6.6	6381784.3
	6	13	874968.6
	7	1.2	1470375.5
SWS	8	3.4	2520939.2
	9	2.4	5697720.5
	9	2.6	4537959.9
	9	3.8	2688835.7
	9	6.6	1497573.6
	10	1.8	6089729.8

Fig. 3. Global spectral composition per epoch. Cumulative power was calculated for the entire epoch and the main frequency peaks were saved in a text file (table-like format). *Left*, The output list contains the following information: epoch number, frequency peak (F_{max}) and power. Data was collected from three different behavioral states (AW, REMS, SWS). One epoch per behavioral state was highlighted (*shading*). *Right*, Power spectrum graphs corresponding to each behavioral state. In the *graph inset*, highest frequency peak and its power.

ent subjects analyzed. We can see that individual data are saved together with mean results of the percentage of oscillatory events as well as their latencies per frequency band in each group. Although we analyzed tonic–clonic seizures from 6 animals, the summary tables will only include those subjects in which ≥ 1.5-s-oscillations were detected.

Hippocampus and amygdala spectral synchronization during epileptic seizures was evaluated by measuring the coherence between their LFPs recordings. Fig. 5 illustrates a graph output for the coherence values calculated from 7 different seizure episodes. A bootstrap-derived 95% confidence interval curve, establishing the significance threshold for coherence estimates, was added to the plot together with phase delay values. Significant coherences were shaded in grey. Although most significant coherence frequencies were associated with near-zero degree phase delays, we could also see near-180° synchronizations (Fig. 5; bottom plot, ∼12 Hz). We could also observe similarities in the hippocampus–amygdala spectral synchronization pattern between pairs of seizure episodes (Fig. 5; plots 3–4 and plots 5–6).

4. Discussion

Synchronous oscillatory activity is an important mechanism to coordinate the firing of distributed neuronal populations during behavioral coding. In several neurological disorders, specific oscillatory patterns are altered and may reveal abnormal network functioning (Uhlhaas and Singer, 2006). However, the spectral analysis of large amount of EEG data relies upon the availability of automated methods for the quantification of brain oscillations and their disruptions. Here, we have developed a semi-automated MATLAB toolbox to quantitatively analyze brain oscillatory activity in full-length LFP or EEG recordings obtained from different paradigms (e.g., physiological state transitions, seizures, drug administration, etc.).

The main strength of the current toolbox is that it allows neuroscientists to extract relevant information from electroencephalographic traces, not available by pure visual inspection, by combining a set of signal processing strategies. The algorithm works by automatically extracting LFP epochs at user-defined onset times (e.g., locked to behavior, drug injection time, etc.), calculating their time–frequency decomposition using wavelet transform, detecting oscillatory events and calculating linear coherence between two brain areas. In addition, it generates several output files containing numerical data for statistical analysis and graph image files for manuscript presentation. Besides, the toolbox will be of public domain.

4.1. Extracting LFP epochs and discarding artifact-containing epochs

One of the bottlenecks in the analysis of behavior coupled to brain oscillatory activity is the amount of data the experimenter has to deal with. As an example, one usually collects min/h of LFP recordings from several animals/subjects during seizures while their behaviors are recorded. As a result, a set of LFPs

(A)

F_{range}	6 Animals											
1	1	0.64	1	0.90	1	0.89	1	0.20	1	0.92	1	0.83
2	2	0.18	2	0.00	2	0.22	2	0.00	2	0.15	2	0.00
3	3	0.27	3	0.50	3	0.11	3	0.20	3	0.15	3	0.17
4	4	0.27	4	0.50	4	0.11	4	0.20	4	0.08	4	0.00
5	5	0.18	5	0.00	5	0.00	5	0.00	5	0.00	5	0.00
6	6	0.00	6	0.00	6	0.00	6	0.00	6	0.00	6	0.00
7	7	0.00	7	0.00	7	0.00	7	0.00	7	0.00	7	0.00

Mean Percentage of Oscillatory Events per Frequency Range

F_{range}	Mean (%)	SD (%)	n (#animals)
1	73.03	27.99	6
2	18.60	3.44	3
3	23.41	14.10	6
4	23.22	16.82	5
5	18.18	NaN	1
6	0.00	0.00	0
7	0.00	0.00	0

(B)

Mean Latency of Oscillatory Events per Frequency Range

F_{range}	Mean Latency (s)	SD (s)	n (# animais)
1	3.6	1.35	6
2	3.5	2.59	3
3	1.53	1.44	6
4	0.81	0.93	5
5	3.5	NaN	1
6	-1	-1	0
7	-1	-1	0

Fig. 4. Across-subject statistics. Multiple files (usually, one per subject) created during the detection of sustained oscillations can be read to produce a group statistics. Besides containing all the original data from each subject, the output text file contains information on (1) mean percentage of oscillatory events ≥1.5 s and (2) mean latency of these events per frequency band. Here, we show a fragment of the output file with the analysis of 6 animals, in five frequency bands. In (A), percentage of oscillatory events in each of the 6 subjects (*upper*) and the total mean percentage (*bottom*). In (B) mean latency of oscillatory events for all subjects. NaN, −1: no data available for analysis. Input parameter: **thre** = 1.5 s.

and timetables of annotated behaviors should be pre-analyzed in order to have behaviorally relevant LFP epochs selected and organized. In addition, selected epochs must undergo artifact rejection before the analysis proceeds. The *epoch_select* and *epoch_display* routines help the experimenter extract user-defined epochs based on a behavioral annotation timetable and then, display all LFP segments on the computer screen for visual inspection and artifact rejection. Numerous epochs can be displayed at once. Of note, visual inspection is a very efficient method for the exclusion of major movement artifacts, though it is not reliable for EEG-like and small amplitude graph artifacts. In such cases, other methods should be applied (Iriarte et al., 2003).

4.2. Time–frequency analysis

Different from the usual STFT that uses sine and cosine waves, the spectral representation of the signal (i.e., epoch) is generated by a wavelet transform that uses a set of wavelets (Torrence and Compo, 1998). With the use of wavelets, a better trade-off between frequency and time resolution in time is obtained. The strategy adopted for the detection of oscillatory events in short LFP epochs was based on the binarization of their time–frequency spectral decomposition using wavelet analysis. The approach relies on the assumption that the binarization process will keep oscillations of higher relative spectral power and discard weaker oscillations. The advantage of this approach is that it is simple and fast. However, the method is very sensitive to high amplitude artifacts and the TFR spectral range. Artifacts will show up as hot spots in the TFR image overshadowing genuine oscillations, whereas high frequency oscillations (≥20 Hz) can be underestimated if TFR images are calculated in broad frequency ranges (e.g., 1–100 Hz) due to their relative low power. To overcome these limitations, one should (1) carefully remove epochs containing artifacts and (2) split the TFR range into two or more frequency bands (e.g., 1–20 Hz; 20–40 Hz) during the

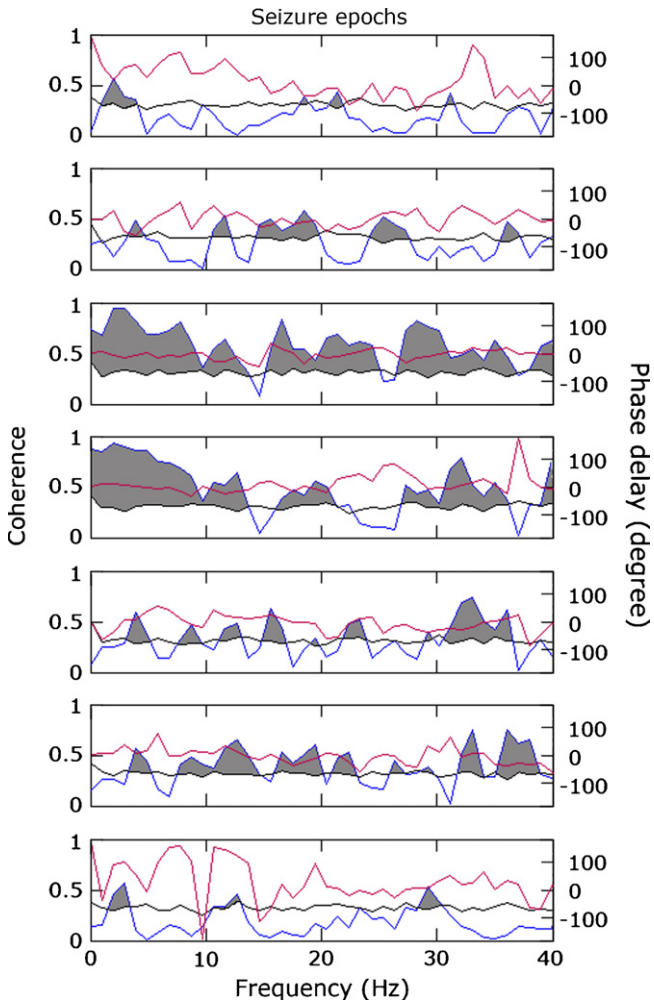

Fig. 5. Coherence analysis of individual epochs. Hippocampus–amygdala synchronization during episodes of audiogenic seizures was estimated by calculating coherence at several frequencies. Here we used 200 bootstrap iterations and a 95% confidence interval to calculate the significance threshold for coherence. *Dark grey*, coherence values. *Light grey*, phase delay values. *Black*, significance threshold. *Grey shading*, coherence values above the significance threshold. Phase difference (phase delay) between hippocampus and amygdala LFPs was plotted on the right *y*-axis (−180 to +180°). Graphs assembled from individual output graphs generated by the software. Input parameters: **boot** = 200; F_s = 500 Hz; **ci** = 0.95.

analysis. Following these procedures, we are safe to apply the algorithm for oscillation detection. A sliding window detection algorithm is applied to obtain oscillatory events lasting ≥600 ms in up to seven frequency bands.

4.3. Brain oscillations

It is postulated that brain oscillatory activity is an important mechanism for information processing and functional binding of distributed neuronal ensembles during cognitive performance. For instance, theta oscillations during exploratory behavior in rats are thought to play important role in space mapping and memory through timing of neuronal firing activity (Buzsaki, 2002). The beta (15–20 Hz) and gamma (25–90 Hz) bands have been implicated in visual working memory processes in monkeys and humans (Pesaran et al., 2002; Tallon-Baudry et al., 2001). The availability of automated methods for quantification of oscillatory and synchronization patterns stimulate the application of such tools in the investigation of meaningful field oscillatory patterns. In such, the computation of coherence is a powerful mathematical tool able to determine spectral synchronization between brain sites.

Herein, we implemented the calculation of linear coherence between pair of EEG time series to measure the degree of oscillatory synchronization. In addition, confidence intervals derived from surrogated data estimates are calculated as a way to reduce spurious high coherence values. One important aspect is that the coherence method used in the toolbox applies STFT to compute the spectrogram of the signal. Therefore, this method is susceptible to the standard limitations of STFT algorithms, such as its dependency on chosen frequency bands, temporal resolution and the sampling rate of the data.

Acknowledgements

We would like to thank Artur Fernandes, Franco Rossetti, Maira Licia Foresti, Marcelo Cairrão Araujo Rodrigues and Orfa Yineth Galvis-Alonso for their comments and suggestions during the development of the algorithm. We also thank Flávio del Vechio and José Antônio Cortes de Oliveira for their technical expertise. The work was supported by grants from FAPESP, CNPq, PRONEX and CAPES-PRODOC.

References

Buzsaki G. Theta oscillations in the hippocampus. Neuron 2002;33:325–40.
Cantero JL, Atienza M. The role of neural synchronization in the emergence of cognition across the wake-sleep cycle. Rev Neurosci 2005;16:69–83.
Challis RE, Kitney RI. Biomedical signal processing (in four parts). Part 3. The power spectrum and coherence function. Med Biol Eng Comput 1991;29:225–41.
Dal-Cól ML, Terra-Bustamante VC, Velasco TR, Oliveira JA, Sakamoto AC, Garcia-Cairasco N. Neuroethology application for the study of human temporal lobe epilepsy: from basic to applied sciences. Epilepsy Behav 2006;8:149–60.
Doretto MC, Fonseca CG, Lobo RB, Terra VC, Oliveira JA, Garcia-Cairasco N. Quantitative study of the response to genetic selection of the Wistar audiogenic rat strain (WAR). Behav Genet 2003;33:33–42.
Drongelen WV. Signal processing for neuroscientists: an introduction to the analysis of physiological signals. 1st ed. Academic Press; 2006. p. 227.
Dutra Moraes MF, Galvis-Alonso OY, Garcia-Cairasco N. Audiogenic kindling in the Wistar rat: a potential model for recruitment of limbic structures. Epilepsy Res 2000;39:251–9.
Faes L, Pinna GD, Porta A, Maestri R, Nollo G. Surrogate data analysis for assessing the significance of the coherence function. IEEE Trans Biomed Eng 2004;51:1156–66.
Garcia-Cairasco N, Wakamatsu H, Oliveira JA, Gomes EL, Del Bel EA, Mello LE. Neuroethological and morphological (Neo-Timm staining) correlates of limbic recruitment during the development of audiogenic kindling in seizure susceptible Wistar rats. Epilepsy Res 1996;26:177–92.
Gross J, Kujala J, Hamalainen M, Timmermann L, Schnitzler A, Salmelin R. Dynamic imaging of coherent sources: studying neural interactions in the human brain. Proc Natl Acad Sci USA 2001;98:694–9.
Iriarte J, Urrestarazu E, Valencia M, Alegre M, Malanda A, Viteri C, et al. Independent component analysis as a tool to eliminate artifacts in EEG: a quantitative study. J Clin Neurophysiol 2003;20:249–57.

Jensen O, Gelfand J, Kounios J, Lisman JE. Oscillations in the alpha band (9–12 Hz) increase with memory load during retention in a short-term memory task. Cereb Cortex 2002;12:877–82.

Kaplan D.M., COHERE_BOOTSTRAP_SIGNIF_LEVEL—Simple Bootstrap to Estimate Significance Level Coherence, Gnu Public Library (GPL), 2004.

Makeig S, Debener S, Onton J, Delorme A. Mining event-related brain dynamics. Trends Cognit Sci 2004;8:204–10.

Otsu N. A threshold selection method from gray-level histograms. IEEE Trans Syst Man Cyber 1979;9:62–6.

Paxinos WC. The rat brain in stereotaxic coordinates. 3rd ed. San Diego: Academic Press; 1997.

Pesaran B, Pezaris JS, Sahani M, Mitra PP, Andersen RA. Temporal structure in neuronal activity during working memory in macaque parietal cortex. Nat Neurosci 2002;5:805–11.

Romcy-Pereira RN, Garcia-Cairasco N. Hippocampal cell proliferation and epileptogenesis after audiogenic kindling are not accompanied by mossy fiber sprouting or Fluoro-Jade staining. Neuroscience 2003;119:533–46.

Steriade M. Synchronized activities of coupled oscillators in the cerebral cortex and thalamus at different levels of vigilance. Cereb Cortex 1997;7:583–604.

Tallon-Baudry C, Bertrand O, Delpuech C, Permier J. Oscillatory gamma-band (30–70 Hz) activity induced by a visual search task in humans. J Neurosci 1997;17:722–34.

Tallon-Baudry C, Bertrand O, Fischer C. Oscillatory synchrony between human extrastriate areas during visual short-term memory maintenance. J Neurosci 2001;21:RC177.

Torrence C, Compo G. A practical guide to wavelet analysis. Bull Am Meteor Soc 1998;79:61–78.

Uhlhaas PJ, Singer W. Neural synchrony in brain disorders: relevance for cognitive dysfunctions and pathophysiology. Neuron 2006;52:155–68.

Zoubir AM, Iskander DR. Bootstrap techniques for signal processing. 1st ed. Cambridge University Press; 2004. p. 232.